

Voltage stability improvement of power system using a shunt capacitor

Masahiro Furukakoi¹, Tomonobu Senju¹ and Toshihisa Funabashi²

¹ Department of Electrical and Electronics Engineering University of the Ryukyus
 1 Senbaru Nishihara-cho Nakagami Okinawa 903-0213 Japan

Phone/Fax number:+81-98-895-8686, e-mail: e125511@gmail.com, b985542@tec.u-ryukyu.ac.jp

² Institute of Materials and Systems for Sustainability (IMaSS) NAGOYA UNIVERSITY
 Furo-cho, Nagoya, 464-8603(Japan)

Phone/Fax number:+81-52-789-2098, e-mail:funabashi@esi.nagoya-u.ac.jp

Abstract. Due to the deregulation of the electricity market, increasing demand approaching transmission capacity, and the endeavor for economic benefits, the power system is recently placed under more severe operating conditions than ever before. Therefore, voltage stability analysis is a major concern in power system planning and operation. This paper proposes a method to improve the voltage stability of the power system by using the active and reactive power information of the transmission line in accordance with the voltage stability index. Installing a bank of shunt capacitors at the load substation in order to inject the proper amount of reactive power can improve the voltage stability of the system as shown by simulations.

Key words

voltage collapse, voltage stability index, shunt capacitor, smart grid, IEEE 5 Bus system

1. Introduction

Recent liberalization of the power market combined with growing concern about of the depletion of energy resources has led to an increase in the introduction of solar power generation within the electric power grid. Moreover, the move to all electric systems in the interest of economic benefits results in an increase in demand, causing the power system to operate near power transmission capacity in progressively severe situations[1]. With more efficient use of transmission lines, it is possible that more parts of the power system can be operated near voltage stability limits. As a result the possibility of voltage collapse will increase[2,3]. Therefore, voltage stability analysis is a major consideration in the stable operation of the power system.

Voltage stability has been analyzed in a variety of ways. Some of the analysis techniques include P-V analysis, which concerns the relationship of the voltage and active power in the transmission system, and Q-V analysis, which concerns the relationship of the voltage and reactive power[4-11]. Proposed indicators of voltage stability include finding the change in active and reactive power with respect to the change in voltage from the P-V and Q-V characteristics, the proximity of the high and low voltage vectors from the PV characteristics, and the voltage

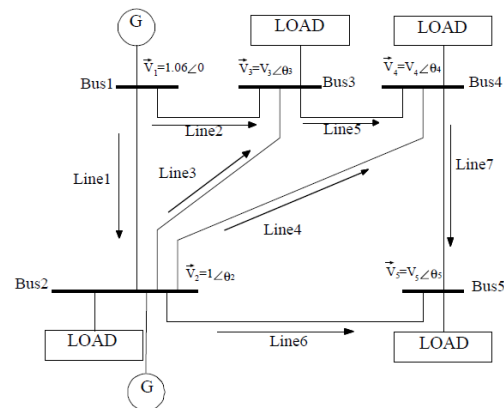


Fig. 1. IEEE 5 Bus System model.

stability margin of the active power that can be consumed by the load. There has been little work done with regards to voltage stability considering both the active and reactive power at the same time because analysis becomes difficult. However, it is expected that accurate voltage stability analysis can be performed considering both the active and reactive powers simultaneously. Because active and reactive power are the main values regarding transmission characteristics, the P-Q characteristics, can be considered. We have previously proposed a voltage stability limit index that takes into account the active and reactive power in the transmission [1].

This paper proposes a method to improve the voltage stability of the power system by using the active and reactive power information of the transmission line in accordance with the voltage stability index. Installing a bank of shunt capacitors at the load substation in order to inject the proper amount of reactive power can improve the voltage stability of the system as shown by simulations.

2. Power system model

The model assumed in this paper is shown in Fig. 1. Table 1 shows the initial values in each bus and Table 2 shows the resistance and reactance of each transmission line. The IEEE 5 Bus system [12] is used in this paper.

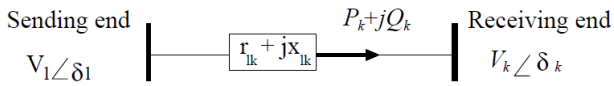


Fig. 2. Transmission line model.

Table 1. IEEE 5-Bus System data

Bus code	Assumed Bus Voltage	Generation		Load	
		MW	MVARs	MW	MVARs
1	1.06+j0.0	0	0	0	0
2	1.0+j0.0	40	30	20	10
3	1.0+j0.0	0	0	45	15
4	1.0+j0.0	0	0	40	5
5	1.0+j0.0	0	0	60	10

Table 2. IEEE 5-Bus System data

Bus code	R/pu	X/pu
1-2	0.02	0.06
1-3	0.08	0.24
2-3	0.06	0.18
2-4	0.06	0.18
2-5	0.04	0.12
3-4	0.01	0.03
4-5	0.08	0.24

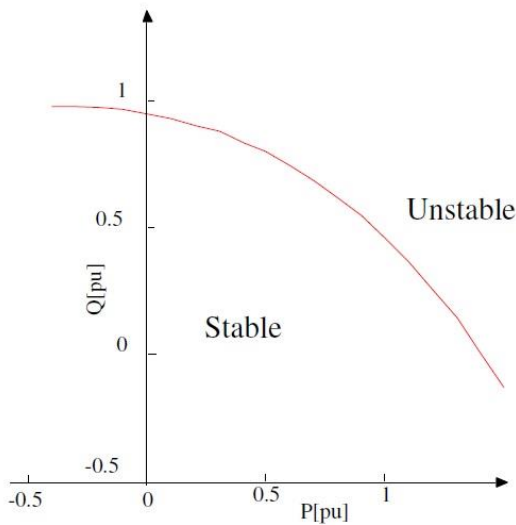


Fig. 3. P-Q characteristics.

3. Voltage stability analysis

In Fig. 2 V_l is the sending end voltage and V_k is the receiving end voltage, P_k is the active power being sent to the receiving side and Q_k is the reactive power being sent. The power flow equation of the two bus system is expressed by the following equation.

$$P_k - Q_k = (V_k \angle \delta_k) \frac{V_l \angle \delta_l - V_k \angle \delta_k}{r_{ik} + jx_{ik}} \quad (1)$$

When separated into real and imaginary parts the equation becomes

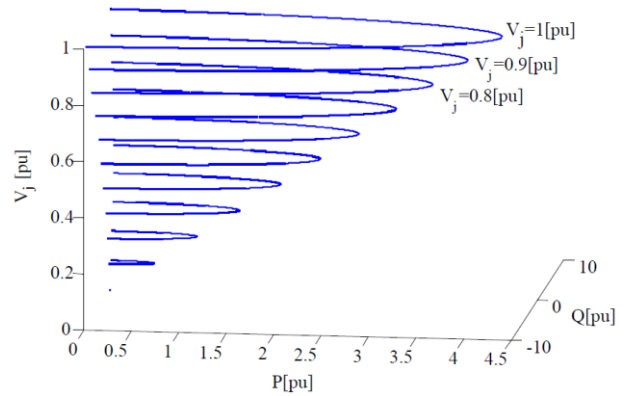


Fig. 4 (P, Q)-V characteristics.

$$(P_k r_{ik} + jx_{ik} Q_k) + j(P_k r_{ik} - jx_{ik} Q_k) = V_l V_k \cos(\delta_l - \delta_k) + jV_l V_k \sin(\delta_l - \delta_k) - V_k^2 \quad (2)$$

Equating both imaginary parts

$$P_k x_{ik} - r_{ik} Q_k = jV_l V_k \sin(\delta_l - \delta_k) \quad (3)$$

Solving for V_k^2 in Eqs. (2) and (3), the following equation is obtained.

$$V_k^2 = \left(r_{ik} P_k + x_{ik} Q_k - \frac{V_l^2}{2} \right) \pm \sqrt{\left(r_{ik} P_k + x_{ik} Q_k - \frac{V_l^2}{2} \right)^2 - (r_{ik}^2 + x_{ik}^2)(P_k^2 + Q_k^2)} \quad (4)$$

Considering sending end voltage and V_k is greater than zero, the following equation is obtained.

$$V_k = \sqrt{\left(r_{ik} P_k + x_{ik} Q_k - \frac{V_l^2}{2} \right) \pm A} \quad (5)$$

$$A = \sqrt{\left(r_{ik} P_k + x_{ik} Q_k - \frac{V_l^2}{2} \right)^2 - (r_{ik}^2 + x_{ik}^2)(P_k^2 + Q_k^2)}$$

There is a limit to possible transmission power for any given time; that power is called the power stability limit and the voltage is called the voltage stability limit. This limit occurs when A in Eq. (5) becomes zero; therefore, the stability limit conditions can be expressed as follows[13].

$$\sqrt{\left(r_{ik} P_k + x_{ik} Q_k - \frac{V_l^2}{2} \right)^2 - (r_{ik}^2 + x_{ik}^2)(P_k^2 + Q_k^2)} = 0 \quad (6)$$

$$Q_k = \frac{\pm \sqrt{x_{ik}^2 V_l^4 + r_{ik}^2 V_l^4 - 4x_{ik}^2 r_{ik} V_l^2 P_k - 4r_{ik}^3 V_l^2 P_k} + 2x_{ik} r_{ik} P_k - x_{ik} V_l^2}{2r_{ik}^2} \quad (7)$$

The P-Q characteristics of the power stability limit from Eqn. (7) are shown in Fig. 3. From Eqns. (6) and (7), the relationship between V_l and P_k at the voltage stability limit is shown as follows.

$$V_k = \sqrt{\left(r_{ik} P_k \pm B - \frac{V_l^2}{2} \right)} \quad (8)$$

$$B = x_{ik} \frac{\sqrt{x_{ik}^2 V_l^4 + r_{ik}^2 V_l^4 - 4x_{ik}^2 r_{ik} V_l^2 P_k - 4r_{ik}^3 V_l^2 P_k} + 2x_{ik} r_{ik} P_k + x_{ik} V_l^2}{2r_{ik}^2}$$

From Eq. (8), the (P, Q)-V characteristics of a stable power limit is shown in Figs. 4 and 5.

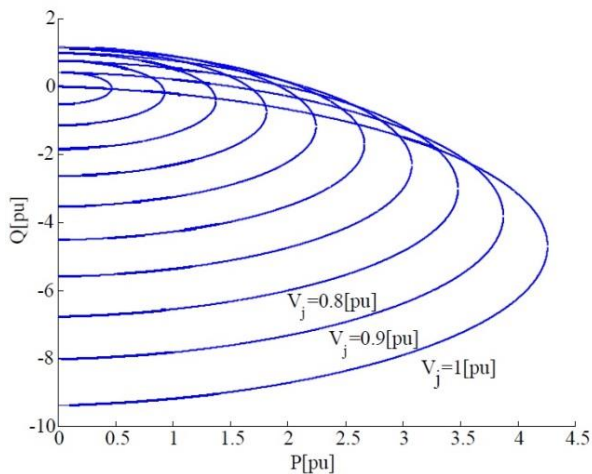


Fig. 5. (P, Q)-V characteristics.

4. Voltage stability index

From the current point $K(P_o, Q_o)$, an unstable point on the curve from Equation (6) $C(X, Y)$ is obtained using Lagrange multipliers. Equation (6) is obtained as follows.

$$C = \left(r_{lk} P_k + x_{lk} Q_k - \frac{V_l^2}{2} \right)^2 - (r_{lk}^2 + x_{lk}^2) (P_k^2 + Q_k^2) = 0 \quad (9)$$

The distance between the current point K and the nearest point of voltage instability C , is a the function $f(X, Y)$ and the minimum of f^2 .

$$f^2 = (X - P_o)^2 + (Y - Q_o)^2 \quad (10)$$

The following equation is obtained by using Lagrange multipliers.

$$F(X, Y, \lambda) = f^2(X, Y) - \lambda C(X, Y) \quad (11)$$

$$F(X, Y, \lambda) = (X - P_o)^2 + (Y - Q_o)^2 - \lambda \left(\left(r_{lk} X + x_{lk} Y - \frac{V_l^2}{2} \right)^2 - (r_{lk}^2 + x_{lk}^2) (X^2 + Y^2) \right) \quad (12)$$

Taking the partial differential equation for X, Y, λ above the following equation is obtained.

$$2X - 2P_o - \lambda \left(2 \left(r_{lk} X + x_{lk} Y - \frac{V_l^2}{2} \right) r_{lk} - 2(r_{lk}^2 + x_{lk}^2) X \right) = 0 \quad (13)$$

$$2Y - 2Q_o - \lambda \left(2 \left(r_{lk} X + x_{lk} Y - \frac{V_l^2}{2} \right) x_{lk} - 2(r_{lk}^2 + x_{lk}^2) Y \right) = 0 \quad (14)$$

$$- \left(r_{lk} X + x_{lk} Y - \frac{V_l^2}{2} \right) + (r_{lk}^2 + x_{lk}^2) (X^2 + Y^2) = 0 \quad (15)$$

The values of X, Y, λ are obtained by simultaneously solving equations (13)~(15). Using these points, the nearest operating point is determined. In this paper, $\Delta P, \Delta Q$ denote the distance to the nearest point from the operating point as the voltage stability index.

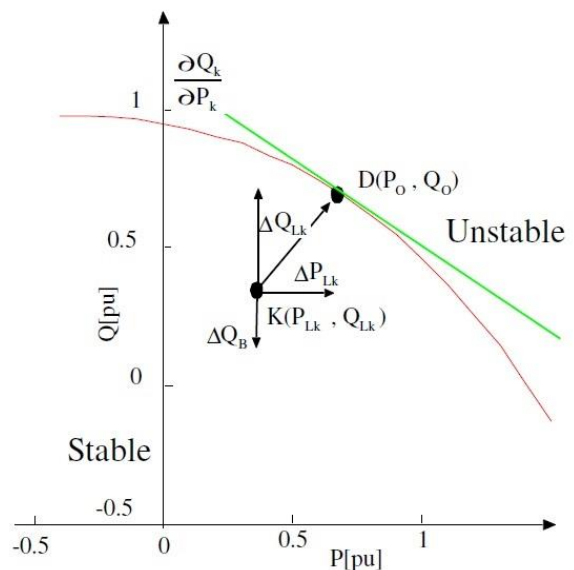


Fig. 6. P-Q characteristics.

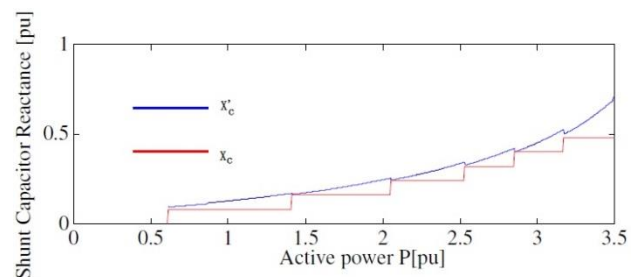


Fig. 7. Shunt Capacitor control.

The voltage stability index for the power transmission line $l-k$ is calculated as the shortest distance from the current operating point to the P-Q voltage stability limit curve. These are demarcated as ΔP and ΔQ and the Critical Boundary Index (CBI) can be evaluated as follows:

$$CBI_{lk} = \sqrt{\Delta P_{lk}^2 + \Delta Q_{lk}^2} \quad (16)$$

Here, 'l' is the sending end bus number, 'k' is the receiving end bus number. The CBI can be used as an index of voltage stability of the transmission line. The voltage stability of the given transmission line worsens as the CBI approaches zero [1].

5. Shunt Capacitor Control Method

The following is the proposed control method aimed at improving the voltage stability by using shunt capacitors housed in the substation. Fig. 6 shows the operating point $K(P_{LK}, Q_{LK})$ and the closest point $D(P_o, Q_o)$ on the stability limit curve. The tangent of the curve at point D is calculated as follows: P_{LK} and Q_{LK} are the active and reactive power flowing through line k . Q_k is derived using Equation (3), as shown in Equation (17).

$$Q_k = \frac{\pm \sqrt{x_{lk}^2 V_l^4 + r_{lk}^2 V_l^4 - 4x_{lk}^2 r_{lk} V_l^2 P_k - 4r_{lk}^2 V_l^2 P_k}}{2r_{lk}^2} + \frac{2x_{lk} r_{lk} P_k - x_{lk} V_l^2}{2r_{lk}^2} \quad (17)$$

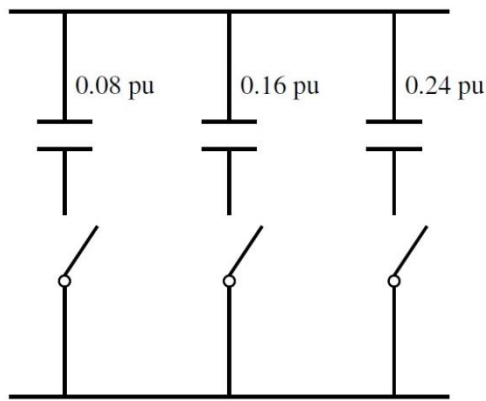


Fig. 8. Shunt Capacitor.

Table 3. Simulation conditions

	Simulation conditions
Case 1	The active power of bus 5 is increased until a voltage collapse occurs.
Case 2	This case is similar to Case 1; however, shunt capacitor compensation is utilized.
Case 3	The active power at buses 2, 3, 4, and 5 is increased at a rate of λ until a voltage collapse occurs.
Case 4	This case is similar to Case 3; however, shunt capacitor compensation is utilized.

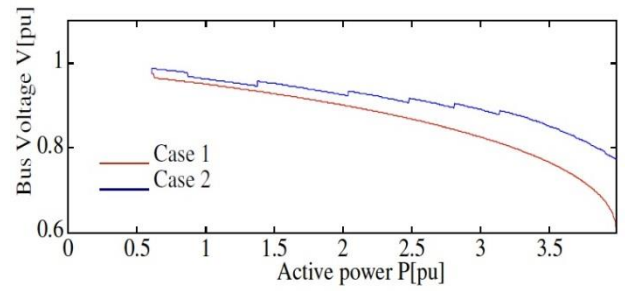
Equation (18) shows the partial differential of Equation (17).

$$\frac{\partial Q_k}{\partial P_k} = \frac{\frac{-2x_{lk}^2 r_{lk} V_l^2 - 2r_{lk}^3 V_l^2}{\sqrt{x_{lk}^2 V_l^4 + r_{lk}^2 V_l^4 - 4x_{lk}^2 r_{lk} V_l^2 P_k - 4r_{lk}^2 V_l^2 P_k}} + 2x_{lk} r_{lk}}{2r_{lk}^2} \quad (18)$$

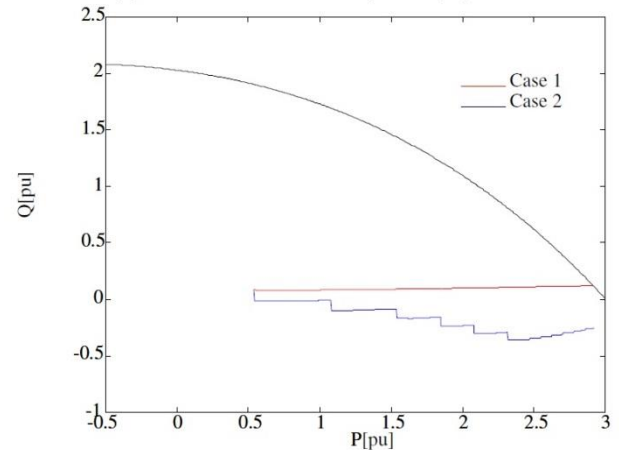
Substituting P_0 for P_k gives the tangent of the voltage stability limit curve at point $D(P_0, Q_0)$. Using the tangent of point D , the necessary reactive power from the shunt capacitor is decided. The voltage stability margin decreases as the steepness of the tangent line increases. As the tangent increases, the amount of required reactive power ΔQ_c increases. The required reactance of the shunt capacitors is calculated using Equation (19).

$$X'_c = \frac{\Delta Q_c}{V_k^2} \quad (19)$$

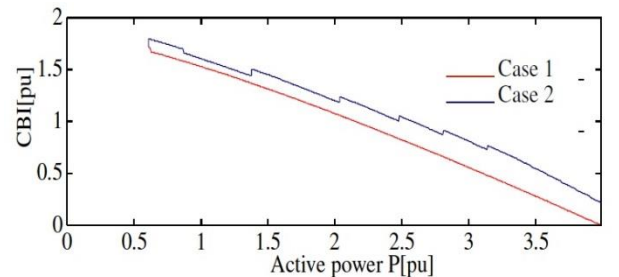
Fig. 8 shows the model of the shunt capacitor connected to each bus. This shunt capacitor can switch to a total of 7 patterns. The actual reactance of the shunt capacitor compared to the necessary reactance X'_c is shown in Fig. 7.



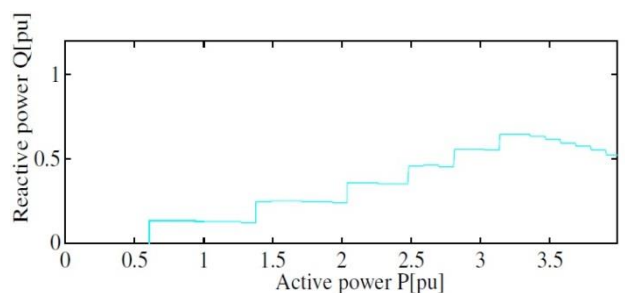
(a) Bus 5 voltage



(b) (P, Q) characteristics (line 6).



(c) Voltage stability index (line 6)



(d) Amount of shunt capacitor compensation (Bus 5)

Fig. 9. Simulation results(Case 1, 2)

6. Simulation results

In order to verify the effectiveness of the proposed method simulations of four scenarios were carried out. The details of these scenarios are shown in Table 3. Below are the results of the simulations.

The results of Cases 1 and 2 are shown in Fig. 9. Fig. 9(a) shows the voltage of Bus 5 as a function of load active power. The relation between active power and

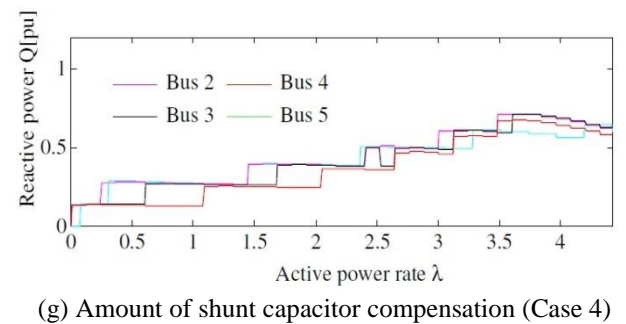
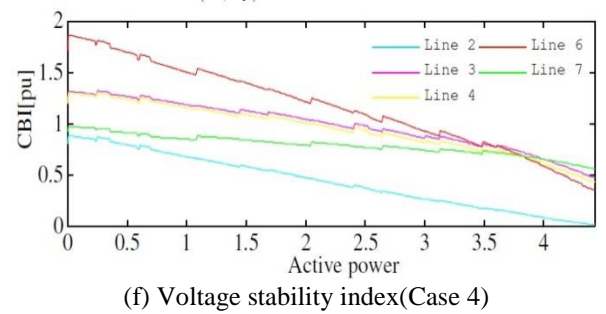
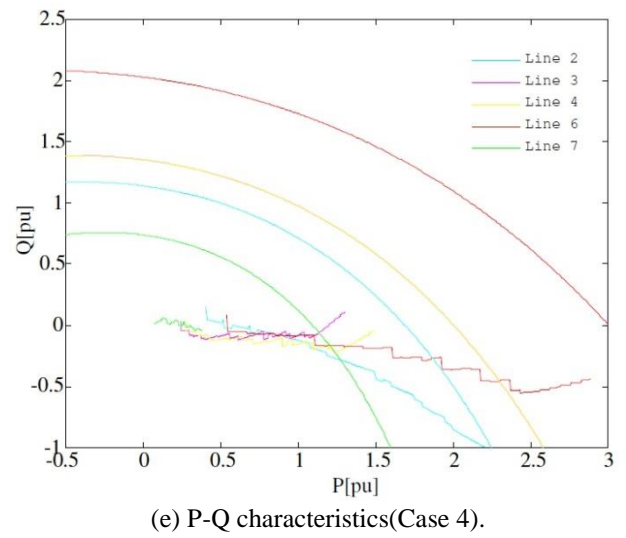
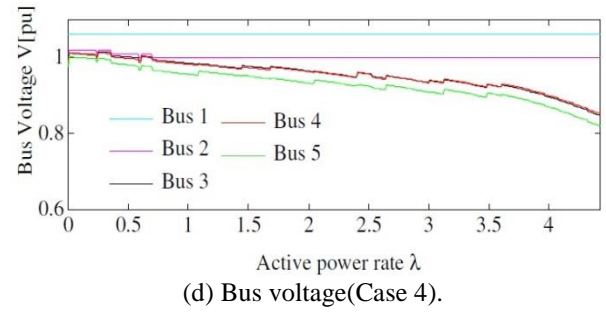
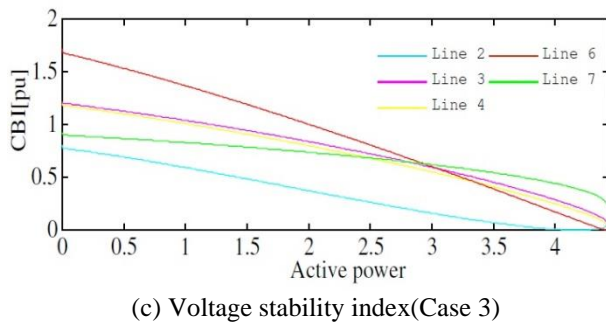
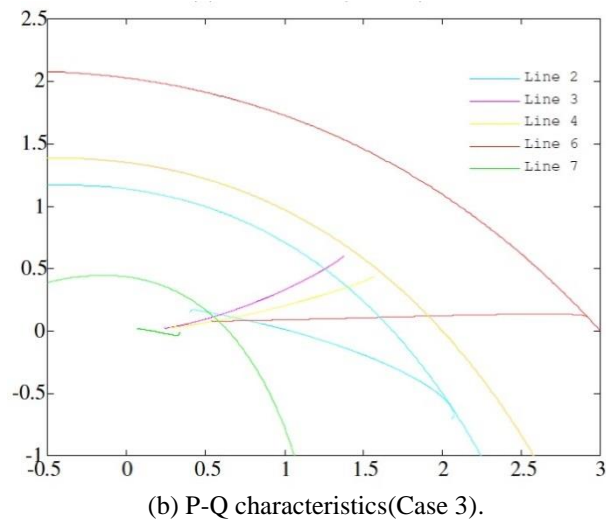
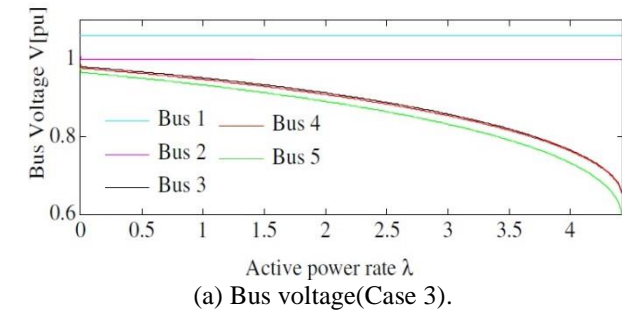


Fig. 10 Simulation results(Case 3, 4)

voltage, that the voltage drops as the load active power increases, can be easily seen in this figure. The PQ characteristics of line 6 are shown in Fig. 9(b). It can be seen that as the load active power increases, the active and reactive power flowing through the line also increases. As a result, the distance between the operating point and the voltage stability curve decreases. In Case 1, there is no shunt capacitor compensation, so the operating point moves above the voltage stability limit curve; thus, a voltage collapse occurs.

Fig. 9(c) shows the critical boundary index (CBI). At the occurrence of the voltage collapse, the CBI is equal to zero. Fig. 9(d) shows the amount of shunt capacitor compensation for Case 2. As active power increases, the compensating reactive power must also be increased to ensure the security of the system. As seen in Fig. 9(b), from the compensation provided by the shunt capacitor, the operating point is kept safely far away from the voltage stability limit curve. Therefore, through the use of a shunt capacitor, the system is protected from voltage sags and voltage collapse.

Fig. 10 shows the results for Cases 3 and 4. Fig. 10(a) shows the voltage of all buses as functions of load active power. Here as well, the relation between active power and voltage, can be easily seen. The PQ characteristics of lines 2, 3, 4, 6 and 7 are shown in Fig. 10(b). When the distance between the operating point of line 6 and the voltage stability limit curve reaches 0, a voltage collapse occurs. Fig. 10(c) shows the CBI of lines 2, 3, 4, 6 and 7. As the active power of each load increases the voltage stability margin decreases. Fig. 10(g) shows the amount of shunt capacitor compensation for Case 4. As active power increases, the compensating reactive power must also be increased to ensure the security of the system. As seen in Fig. 10(e), from the compensation provided by the shunt capacitor, the operating point is kept safely far away from the voltage stability limit curve. In Fig. 10(f), comparing with Case 3 the voltage stability index is very high. The scenario of Cases 3 and 4 are similar; however, in Case 4, shunt capacitor compensation is used, whereas it is not used in Case 3, thus a voltage collapse occurs. The system in Case 4 is kept safe through the use of the shunt capacitors.

7. Conclusion

On the basis of the critical boundary index (CBI), installing shunt capacitors in the power system allows the injection of reactive power when loads are increased or a fault occurs, and this makes it possible to improve the voltage stability of the power system as shown by the simulation results. It is possible to improve the results of this study by applying an optimization technique to find the most beneficial shunt capacitor installation locations as well as the most beneficial amount of injected reactive power.

References

[1] Masato Tachibana, Michael Damien Palmer, Tomonobu Senjyu and Toshihisa Funabashi, "Voltage Stability Analysis and (P,Q)-V Characteristics of Multi-bus System," *CIGRE AORC Technical Meeting 2014*, .
 [2] Yuan-Kang Wu, "A novel algorithm for ATC calculations and applications in deregulated electricity markets," *International Journal of Electr Power and Energy Systems*, vol. 29, Issue 10, pp. 810-821, 2007.

[3] Ajarapu V. and Lee B., "Bibliography on voltage stability," *IEEE Trans. on Power System*, vol.13, Issue 1, pp. 115-125, 1998.
 [4] Taylor CW, "Power system voltage stability," New York: McGraw-Hill; 1994.
 [5] Leonardi B and Ajarapu V, "An Approach for Real Time Voltage Stability Margin Control via Reactive Power Reserve Sensitivities," *IEEE Trans. on Power System*, vol. 28, Issue 2, pp. 615-625, 2013.
 [6] Corsi S. and Taranto G.N., "Voltage Instability -the Different Shapes of the "Nose"," *Bulk Power System Dynamics and Control - VII. Revitalizing Operational Reliability, 2007 iREP Symposium*, pp. 1-16, 2007.
 [7] Li Lin, Junbing Wang, and Wenzhong Gao, "Effect of load power factor on voltage stability of distribution Substation," *IEEE Power and Energy Society General Meeting*, pp.1-4, 2012.
 [8] Hiroshi Okamoto, Ryuya Tanabe, Yasuyuki Tada, and Yasuji Sekine, "Method for Voltage Stability Constrained Optimal Power Flow (VSCOPF)," *IEEE Transactions on Power and Energy* vol. 121, 8 Issue 12, pp. 1670-1680, 2001.
 [9] M. Glavic, M. Lelic, D. Novosel, E. Heredia, and D.N. Kosterev, "simple computation and visualization of voltage stability power margins in real-time", *Transmission and Distribution Conference and Exposition, 2012 IEEE PES*, pp. 1-7, 2012.
 [10] O.A. Mousavi, M. Bozorg, A. Ahmadi-Khatir, and R. Cherkaoui, "Reactive power reserve management: Preventive countermeasure for improving voltage stability margin," *IEEE Power and Energy Society General Meeting, 2012* pp. 1-7, 2012.
 [11] H. Kazari, A. Abbaspour-Tehrani Fard, A.S. Dobakhshari, and A.M. Ranjbar, "Voltage stability improvement through centralized reactive power management on the Smart Grid," *Innovative Smart Grid Technologies, 2012 IEEE PES*, pp. 1-7, 2012.
 [12] P. Srikanth, O. Rajendra, A.Yesuraj, M.Tilak, "Load Flow Analysis Of Ieee14 Bus System Using MATLAB," *International Journal of Engineering Research and Technology*, vol. 2, Issue 5, pp. 149-155, 2013.
 [13] B.Venkatesh, Alex Rost, Riuchen Chang, "namic Volt age Collapse Index-Wind Generator Application", *IEEE Trans. on Power Delivery*, vol. 22, Issue 1, pp. 90-94, 2007.